International Journal of Engineering

Journal Homepage: www.ije.ir

Mechanical Properties Analysis of Bilayer Euler-Bernoulli Beams Based on Elasticity Theory

Z. Zhang*[a], C. Zhang[b]

[a] *Zhejiang Sci-Tech University, Hangzhou, Zhejiang Province – 928, No.2 Avenue, Xiasha, China*
[b] *Minmetals Yingkou Medium Plate CO., LTD, Yingkou, Liaoning Province, China*

PAPER INFO

Paper history:
Received 11 March 2020
Received in revised form 04 April 2020
Accepted 12 June 2020

Keywords:
Bilayer Beam
Euler-Bernoulli Hypothesis Model
Natural Frequency
Static Deflection

ABSTRACT

This paper analyzes the effects of structures and loads on the static bending and free vibration problems of bilayer beams. Based on static mechanical equilibrium and energy equilibrium, the static and dynamic governing equations of bilayer beam are established. It is found that the value of the thickness ratio has a significant effect on the static and dynamic responses of the beam, and the structure factors have their own critical value. When the value of the relative thickness is lower than its critical value or the length thickness ratio is greater than its critical value, the static and dynamic responses of the beam increase obviously. The results reveal that a critical value exists in bilayer beam, the value has noticeable influence on the mechanical properties of bilayer beams. Therefore, investigators should predict the critical structures accurately, when they design the bilayer beam.

doi: *10.5829/ije.2020.33.08b.25*

NOMENCLATURE

M	Bending moment (N·mm)	$w(x,t)$	Amplitude (mm)
F_s	Shear force (N)	La	Lagrange's function
q	Uniformly distributed load (N/mm)	k	The stiffness of an elastic foundation
L	Beam length (mm)	u_i	Displacement vector
h	Thickness (mm)	$m=E_1/E_2$	Ratio of elasticity modulus
b	Width (mm)	**Greek Symbols**	
w	Deflection (mm)	$\boldsymbol{\sigma}$	Stress tensor
E	Material elastic modulus (GPa)	ε	Strain tensor
I	Second moment of cross-sectional area (mm^4)	ω	Natural frequency (Hz)
d	Distance from the neutral layer to the bottom layer	ξ	Relative thickness
A	Cross-sectional area of the beam (mm^2)	υ	Poisson's ratio
$\boldsymbol{U}$	Strain energy (J)	ρ	Density (kg/m^3)
$\boldsymbol{V}$	Work done by the external forces (J)	**Subscripts**	
$\boldsymbol{T}$	Kinetic energy(J)	e	Bilayer beam

1. INTRODUCTION

Beams are one of the major structures used widely in mechanical systems, such as energy harvesters [1], sensors [2] and the construction industry [3]. Haghpanah [4] and Laminou [5] found that the structure size and load would have a significant impact on the mechanical properties of the mechanical systems. Hence, a lot of work has been undertaken to explore the mechanical properties of beams.

*Corresponding Author Institutional Email: *zzj512682701@126.com* (Z. Zhang)

Scarpa [6] and Damanpack [7] analyzed the elastic mechanical properties of a single layer beam model. However, with the research continuing in-depth, many researchers have found that the power output of mechanical systems applied to composite beam structures are higher than that on monolayer beam structures. Kok et al. [8] found that the multilayer piezoelectric cantilever beam has a higher power output efficiency than monolayer. Chun et al. [9] observed that increasing the number of actuator piezoelectric layer can improve the actuator power output effectively.

To predicate the beams mechanical properties accurately, some researchers use the business software [10-11]. For example, Al-Qasem et al. [12] calculated the shear stress in a cantilever beam by ANSYS software. However, theoretical basis is lacked in this approach. Therefore, many researchers used a mathematical calculation which are based on mechanical theory to study the mechanical properties of beams. For example, Lotfavar [13] and Alashti [14] applied Hamilton's variational principle to establish the governing equations of monolayer beams. Torabi et al. [15] investigated free vibration of a beam in variational iteration method which is based on mechanical theory. JafarSadeghi-Pournaki [16] analyed static deflection problem of beams by Galerkin.

Physical properties of the materials in each layer in the multilayer beam vary. Therefore, to calculate the location of neutral axis of the multilayer beam, an alternative two-variable method has been used to solve the bending problem of bilayer beam subjected to external moments and internal stresses by Zhang et al. [17]. Rastegarian and Sharifi [18] studied inter-story drifts in conventional RC multilayer moment frames. Based on the elastic equivalent relationship, T-J. Subsequently, Zhang et al. [19] analyzed the elastic bending deformation of bilayer beams by alternative two variable methods. Hsueh et al. [20] presented a new analytical model to obtain the mechanical properties of the multilayer beams. They also studied the multilayer problems of stress distribution [21] and elastic thermal stresses in two dissimilar materials [22]. Although, they have taken a lot of work on the mechanical properties of the multilayer beams, but most cases they neglected the effect of the structures on the mechanical properties of the multilayer beams.

In summary, based on the classical elastic theory, the object of this research is to find out the effects of structures and loads on the static bending and free vibration problems of bilayer beams.

The structure of the article is arranged as following; Based on the bilayer Euler-Bernoulli beams elasticity mechanical theory model including static governing equations and dynamic governing equations are established in section 2. In Section 3, the effect of loads and structures on the static and dynamic response of the beam are assessed. Finally, conclusion of this paper appears in Section 4.

2. GOVERNING EQUATION

The two-dimensional schematic diagram of a Euler-Bernoulli beam is shown in Figure 1. The hypothesis of Euler–Bernoulli beam ignores the effect of the centroidal axis rotation angle of the beam. The displacement field is written as:

$$u_x = z\frac{dw(x)}{dx}, u_y = 0, u_z = w(x) \tag{1}$$

where u_x, u_y, u_z are the displacement vector, and $w(x)$ the deflection of the beam.

The beam strain Equation (2) and stress Equation (3).

$$\varepsilon_{xx} = \frac{du_x}{dx} = z\frac{d^2w(x)}{dx^2} \tag{2}$$

$$\sigma_{xx} = Ez\frac{d^2w(x)}{dx^2} \tag{3}$$

The relation between bending moment, shear force and displacement is shown as Equation (4).

$$\begin{cases} M = -EI\dfrac{d^2w}{dx^2} \\ F_s = -\dfrac{d}{dx}\left(EI\dfrac{d^2w}{dx^2}\right) \end{cases} \tag{4}$$

2. 1. Static Theoretical Model

The location of the neutral axis can be calculated by Equation (5) [23], d represents the distance from the neutral layer to the bottom layer.

$$d = \left[1 + \frac{me(1+e)}{1+me}\right]\frac{h_2}{2} \tag{5}$$

where $m=E_1/E_2$, $e=h_1/h_2$, E_1 and E_2 represent the material elastic moduli of layers no.1 and 2, h_1 and h_2 represent the thickness of layers no. 1 and 2. Equation (6) is the equivalent unit length mass equation of the

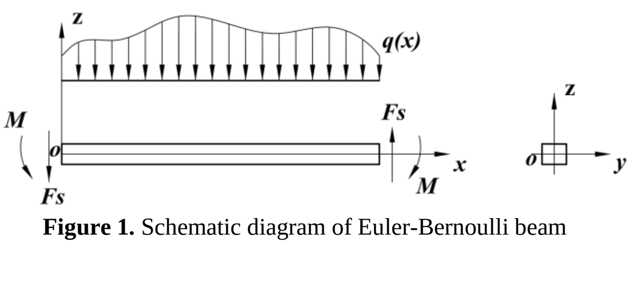

Figure 1. Schematic diagram of Euler-Bernoulli beam

bilayer beam. Equation (7) is the equivalent bending stiffness equation of the bilayer beam.

$$(\rho A)_e = \rho_1 A_1 + \rho_2 A_2 \tag{6}$$

$$\begin{aligned}(EI)_e &= E_1 I_1 + E_2 I_2 + E_1 A_1 \left(h_2 + \frac{h_1}{2} - d \right)^2 \\ &+ E_2 A_2 \left(d - \frac{h_2}{2} \right)^2\end{aligned} \tag{7}$$

where A is the cross-sectional area of the beam and I is the second moment of cross-sectional area.

Inserting Equations (6) and (7) into Equation (4), yields the bilayer beam static governing equation.

$$(EI)_e \frac{d^4 w(x)}{dx^4} = -q(x) - kw(x) \tag{8}$$

Solving Equation (8) then gives:

$$\begin{aligned}w(x) &= C_1 \cos(\beta x)\cosh(\beta x) + C_2 \sin(\beta x)\sinh(\beta x) \\ &+ C_3 \cos(\beta x)\sinh(\beta x) + C_4 \sin(\beta x)\cosh(\beta x) - \frac{q}{k}\end{aligned} \tag{9}$$

where

$$\beta = \left(\frac{k}{4(EI)_e} \right)^{1/4} \tag{10}$$

As shown in Figure 2, the characterized of a cantilever beam is that one end is clamped, the other end is free. The boundary conditions are shown in Equation (11).

$$w(0) = 0, \frac{dw(0)}{dx} = 0, \frac{d^2 w(L)}{dx^2} = 0, \frac{d^3 w(L)}{dx^3} = 0 \tag{11}$$

Substituting Equation (9) into Equation (11), then the value of C_1, C_2, C_3, and C_4 can be obtained.

2. 2. Dynamic Theoretical Model Energy equilibrium is applied to solve the dynamic problem in this paper. The strain energy ***U*** is given by:

$$\mathrm{U} = \frac{1}{2}\int_V \sigma_{ij}\varepsilon_{ij} dV \qquad (i, j = x, y, z) \tag{12}$$

Inserting Equations (2) and (3) into Equation (12), yields the bilayer beam strain energy ***U***:

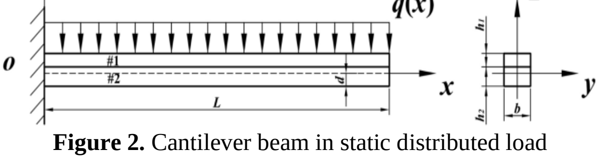

Figure 2. Cantilever beam in static distributed load

$$\boldsymbol{U} = \frac{1}{2}\int_0^L (EI)_e \left(\frac{\partial^2 w(x,t)}{\partial x^2} \right)^2 dx \tag{13}$$

The work done by the external forces ***V*** as shown in Figure 1, reads:

$$\boldsymbol{V} = -\int_0^L q(x,t) w(x,t) dx \tag{14}$$

And the kinetic energy ***T*** can be written as:

$$\boldsymbol{T} = \frac{1}{2}\int_0^L \rho(x) A(x) \left(\frac{\partial w(x,t)}{\partial t} \right)^2 dx \tag{15}$$

By means of Hamiltonian principle, the dynamic governing equation can be determined.

$$\delta \left\{ \int_{t_1}^{t_2} \left(\boldsymbol{T} - \boldsymbol{V} - \boldsymbol{U} \right) dt \right\} = 0 \tag{16}$$

Substituting Equations (13), (14) and (15) into Equation (16), then leads to:

$$\begin{aligned}&\delta \int_{t_1}^{t_2} \int_0^L \left[\frac{1}{2}(\rho A)_e \left(\frac{\partial^2 w(x,t)}{\partial t^2} \right)^2 \right. \\ &\left. - \frac{1}{2}(EI)_e \left(\frac{\partial^2 w(x,t)}{\partial x^2} \right)^2 + q(x,t) w(x,t) \right] dx dt = 0\end{aligned} \tag{17}$$

Lagrange's function:

$$La = \frac{1}{2}\rho A \left(\frac{\partial^2 w(x,t)}{\partial t^2} \right)^2 - \frac{1}{2}(EI) \left(\frac{\partial^2 w(x,t)}{\partial x^2} \right)^2 + qw \tag{18}$$

Through the calculation, Equation (17) can be written as:

$$\begin{aligned}&\int_{t_1}^{t_2} \int_0^L \left[-\left(EI\right)_e w^{(4)} - \rho A \ddot{w} + q \right] \delta w dx dt \\ &- \int_{t_1}^{t_2} \left[\left(EI\right)_e w^{(4)} \delta w \right]_0^L dt - \int_{t_1}^{t_2} \left[\left(EI\right)_e w' \delta w' \right]_0^L dt \\ &+ \int_0^L \left(\dot{w} \delta w \right)_{t_1}^{t_2} dx = 0\end{aligned} \tag{19}$$

where

$$w' = \frac{\partial w}{\partial x}, w^{(3)} = \frac{\partial^3 w}{\partial x^3}, w^{(4)} = \frac{\partial^4 w}{\partial x^4}, \ddot{w} = \frac{\partial^2 w}{\partial t^2} \tag{20}$$

According to Equation (19), without any external force, $q(x,t)$=0, the dynamic governing equation of the bilayer beam will transform as the free vibration Equation (32):

$$(\rho A)_e \frac{\partial^2 w(x,t)}{\partial t^2} + (EI)_e \frac{\partial^4 w(x,t)}{\partial x^4} = 0 \tag{21}$$

where $w(x,t)$ is a function of the coordinate x and time t, and the variable separation approach can be added to solve Equation (21).

$$w(x,t) = W(x) \bullet H(t) \tag{22}$$

Inserting Equation (22) into Equation (21), yields:

$$-\frac{(EI)_e}{(\rho A)_e} \bullet \frac{\frac{d^4W(x)}{dx^4}}{W(x)} = \frac{\frac{d^2H(t)}{dt^2}}{H(t)} \tag{23}$$

where the function variables on both sides of the equal sign is different. Equation (23) can be set up only when both equations are equal to a constant. Suppose the constant equals to $-\omega^2$, the ordinary differential equation of $W(x)$ can be given as:

$$(EI)_e \frac{d^4W(x)}{dx^4} - \omega^2 (\rho A)_e W(x) = 0 \tag{24}$$

Solving Equation (24) then gives amplitude equation:

$$\begin{aligned} W(x) &= C_5 \sin(\gamma x) + C_6 \cos(\gamma x) \\ &\quad + C_7 \sinh(\gamma x) + C_8 \cosh(\gamma x) \end{aligned} \tag{25}$$

where

$$\gamma = \left(\frac{(\rho A)_e \omega^2}{(EI)_e} \right)^{1/4} \tag{26}$$

Then yields the natural frequency ω:

$$\omega = (\gamma L)^2 \sqrt{\frac{(EI)_e}{(\rho A)_e L^4}} \tag{27}$$

The schematic diagram of the cantilever beam in free vibration is shown as Figure 3. Substituting amplitude Equation (25) into the boundary condition of cantilever beam Equation (11), then leads to:

$$\cos(\gamma_i L)\cosh(\gamma_i L) = -1 \tag{28}$$

2. 3. Analytical Flowchart Calculation program for static and dynamic responses is accomplished using MATLAB. The analytical flowchart is shown in Figure. 4.

3. RESULTS AND DISCUSSIONS

To illustrate the static and dynamic responses of bilayer beam, the PZT film / Si substrate bilayer system is considered as an example. In this case, the material constants are: elastic modulus of layer no. 1, E_1=101GPa, elastic modulus of layer no. 2, E_2=168.9GPa, ρ_1=7.5×10^{3}kg/m^3, ρ_2=2.331×10^{3}kg/m^3 [24]. The width is set as b=4h and the length is set as L=200h. h represents total thickness of the beam h=h_1+h_2=0.5×10^{-3}m. The ratio of the thicknesses h_1/h_2 is set to 1/9.

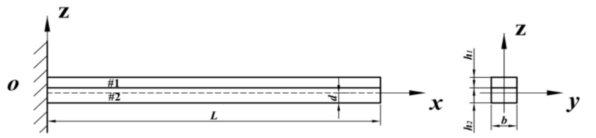

Figure 3. Schematic diagram of the cantilever beam in free vibration

3. 1. Static Responses of Bilayer Beams Effect on the deflection with respect to different loads for a cantilever beam is shown as Figure 5. Under the material and structure dimension remain constant, the static deflection of the cantilever beam increases as the static distributed load increase. The maximum deflection of the cantilever beam is appeared at the free end of the beam (at x=L). In the process of the distributed load increases from 10N/m to 50N/m, the

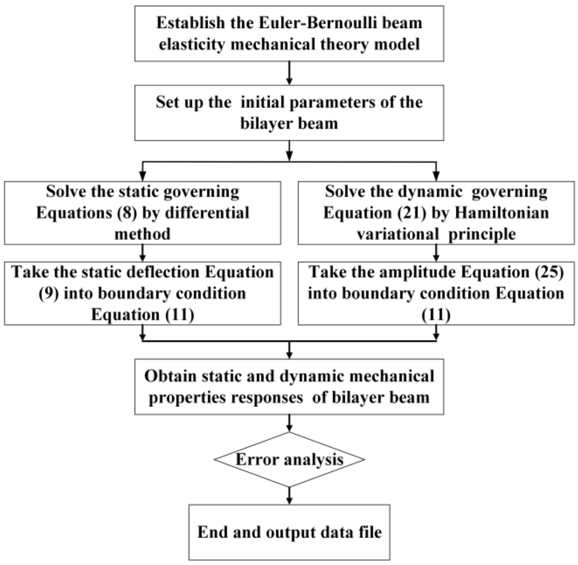

Figure 4. Analytical flowchart of the bilayer beam

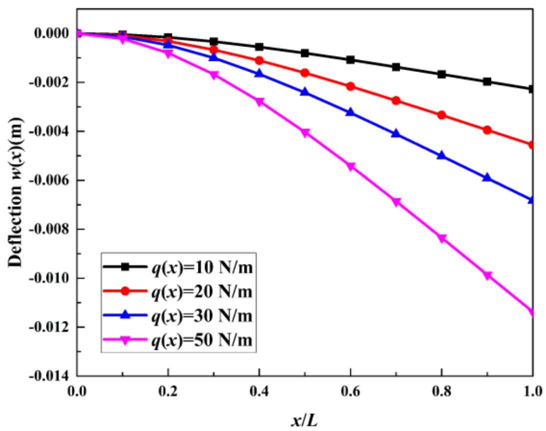

Figure 5. Deflection of the cantilever bilayer beam based on four different distributed load

beam maximum deflection increases from 0.01mm to 0.09mm.

The thickness ratio is an important factor. With the distributed load $q(x)$=20N/m, the effect of the thickness ratio on cantilever beam deflection at $x=L$ is analyzed. From Figure 6, it is found that the cantilever deflection decreases as the increases of the upper layer h_1 thickness proportion with the total thickness remain constant. When the ratio of h_1/h_2 increases from 1 to 8, absolute value of deflection of the cantilever rapidly decreases from 0.053mm to 0.046mm. However, when the thickness ratio increases from 8 to 30, the absolute value of deflection increases only 0.002mm. It is observed that when the thickness ratio of the bilayer cantilever beam exceeds 8, the effect of the thickness ratio on beam deflection can be ignored.

3. 2. Dynamic Responses of Bilayer Beams

The influence of the relative thickness on natural frequency of the cantilever beam, ω, in free vibration is shown in Figure 7. The dimensionless relative thickness

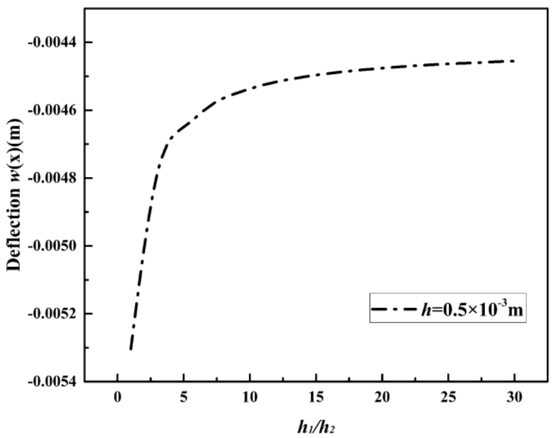

Figure 6. Effect of thickness ratio on cantilever bilayer beam deflection

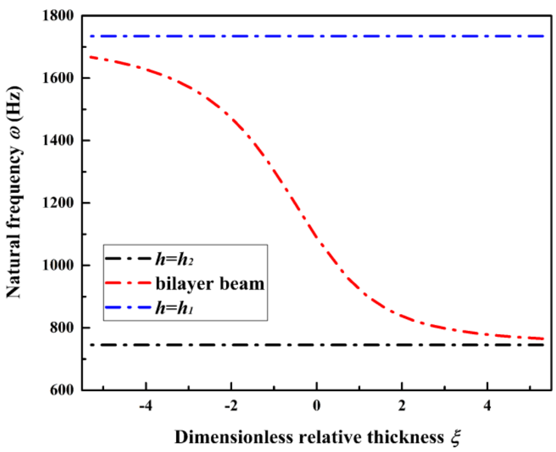

Figure 7. Effect of relative thickness on natural frequency of the cantilever bilayer beam

equation is shown as Equation (43). With the total thickness remains constant, when the value of the relative thickness is larger than 4 (the value of the thickness of layer no. 1 is 17 times greater than the value of layer no. 1), the natural frequency of the bilayer beam is approximately equal to that of the single layer no. 2 beam 744.86 Hz. When the value of the relative thickness is less than -4 (the value of the thickness of layer no. 2 beam is 1/17 times less than the value of layer no. 1), the natural frequency of the bilayer beam is approximately equal to that of the single layer no. 1 beam 1734.4Hz.

$$\xi = \frac{(h_1 - h_2)}{\sqrt{h_1 h_2}} \tag{43}$$

4. CONCLUSIONS

This paper analyzes the static and dynamic problems of the Euler-Bernoulli bilayer beams on the basis of elasticity theory. The static and dynamic governing equations of bilayer beam are established by static mechanical equilibrium and energy equilibrium. It is found that the loads and beam structure have a significant effect on the static and dynamic responses of the bilayer beam. Under the static loads, the deflection increases with the increase of the static load. The thickness ratio and the length thickness ratio of the bilayer beam have their own critical values. When the thickness ratio is less than its critical value or value of the length thickness ratio is higher than its critical value, the static deflection of bilayer beam will change significantly. Under the free vibration, with the increase of the relative thickness, the natural frequency of bilayer beam is gradually transferred from the single layer beam of one material to the single layer beam of another material. When the relative thickness exceeds its critical value, the natural frequency of the bilayer beam is approximately equal to that of the single beam.

5. REFERENCES

1. Wang, L., Ding, J. J., Jiang, Z. D., Jiang, Z. D., Luo, G. X. Zhao, L., Lu, D. J., Yang, X. and Maeda, R., "A packaged piezoelectric vibration energy harvester with high power and broadband characteristics", ***Sensors and Actuators A: Physical***, Vol. 295, (2019), 629-636. DOI: 10.1016/j.sna.2019.06.034
2. Ferraria,M., Alghisi, D., Baù, M. and Ferrari,V., "Nonlinear Multi-Frequency Converter Array for Vibration Energy Harvesting in Autonomous Sensors", in 26th European Conference on Solid-State Transducers (Eurosensors) in Wroclaw Univ Technol, Fac Microsystem Elect & Photon, Krakow, POLAND 2012, Procedia Engineering, Vol. 47, (2012). DOI: 10.1016/j.proeng.2012.09.171
3. Khorramshahi, M. R. and Mokhtari, A., "Automatic

Construction by Contour Crafting Technology", ***Emerging Science Journal***, Vol. 1, No. 4, (2017), 1-28. DOI: 10.28991/esj-2017-01113

4. Haghpanah, F. and Foroughi H., "Size and Shape Optimization of Space Trusses Considering Geometrical Imperfection-Sensitivity in Buckling Constraints", ***Civil Engineering Journal***, Vol. 3, No. 12, (2018), 1314-1326. DOI: 10.28991/cej-030960
5. Laminou, L. M., Liu, Z. J., and Chen, X. H., "Extreme Events design and Mitigation Methods: A Review", ***Civil Engineering Journal***, Vol. 5, No. 6, (2019), 1424-1439. DOI: 10.28991/cej-2019-03091342
6. Scarpa, F., Adhikari, S. and Phani, A. S., "Effective elastic mechanical properties of single layer graphene sheets", ***Nanotechnology***, Vol. 20, No. 6, (2009), 1-11. DOI: 10.1088/0957-4484/20/6/065709
7. Damanpack, A. R., Bodaghi, M., Aghdam, M. M. and Shakeni, M., "On the vibration control capability of shape memory alloy composite beams", ***Composite Structures***, Vol. 110, (2014), 325-334. DOI: 10.1016/j.compstruct.2013.12.002
8. Kok, S. L., White, N. M. and Harris, N. R., "Fabrication and characterization of free-standing thick-film piezoelectric cantilevers for energy harvesting", ***Measurement Science and Technology***, Vol. 20, No. 12, (2009), 1-13. DOI: 10.1088/0957-0233/20/12/124010
9. Chun, D. M., Sato, M. and Kanno, I., "Precise measurement of the transverse piezoelectric coefficient for thin films on anisotropic substrate", ***Journal of Applied Physics***, Vol. 113, No. 4, (2013), 044111.1-044111.19. DOI: 10.1063/1.4789347
10. Alameh, A. H., Gratuze, M. and Nabki, F., "Impact of Geometry on the Performance of Cantilever-Based Piezoelectric Vibration Energy Harvesters", ***IEEE Sensors Journal***, Vol. 22, No. 15, (2019), 10316-10326. DOI: 10.1109/JSEN.2019.2932341
11. Wang, L., Zhao, L. B., Jiang, Z. D., Luo, G. X., Yang, P., Han, X. G., Li, X. and Maeda, R., "High accuracy Comsol simulation method of bimorph cantilever for piezoelectric vibration energy harvesting", ***AIP Advances***, Vol. 9, No. 9, (2019), 095067.1-095067.7. DOI: 10.1063/1.5119328
12. Al-Qasem, I., Hasan, A. R., Abdulwahid, M. Y. and Galobardes, I., "Comparison between Analytical Equation and Numerical Methods for Determining Shear Stress in a Cantilever Beam", ***Civil Engineering Journal***, Vol. 4, No. 2, (2018), 258-265. DOI: 10.28991/cej-030989
13. Lotfavar, A. and Mosalaeifard, A. H., "Three-dimensional Vibration Suppression of an Euler-Bernoulli Beam via Boundary Control Method", ***International Journal of Engineering-Transactions B: Applications***, Vol. 28, No. 5, (2015), 755-763. DOI: 10.5829/idosi.ije.2015.28.05b.14
14. Alashti, R. A, and Abolghasemi, A. H., "A Size-dependent Bernoulli-Euler Beam Formulation based on a New Model of Couple Stress Theory", ***International Journal of Engineering-Transactions C: Aspects,*** Vol. 27, No. 6, (2014), 951-960. DOI: 10.5829/idosi.ije.2014.27.06c.14
15. Torabi, K., Ghassabib, M., Heidari-Rarania, M., and Sharific, D., "Variational Iteration Method for Free Vibration Analysis of a Timoshenko Beam under Various Boundary Conditions" , ***International Journal of Engineering- Transactions A: Basics***, Vol. 30, No. 10, (2017), 1565-1572. DOI: 10.5829/ije.2017.30.10a.18
16. JafarSadeghi-Pournaki, I., Zamanzadeh, M. R., Madinei, H. and Rezazadeh, G., "Static Pull-in Analysis of Capacitive FGM Nanocantilevers Subjected to Thermal Moment using Eringen's Nonlocal Elasticity", ***International Journal of Engineering-Transactions A: Basics***, Vol. 27, No. 4, (2014), 633-642. DOI: 10.5829/idosi.ije.2014.27.04a.15
17. Zhang, N. H. and Chen, J. Z., "Elastic bending analysis of bilayered beams by an alternative two-variable method", ***European Journal of Mechanics, A/Solids***, Vol. 28, No. 2, (2009), 284-288. DOI: 10.1016/j.euromechsol.2008.07.004
18. Rastegarian, S. and Sharifi, A., "An Investigation on the Correlation of Inter-Story Drift and Performance Objectives in Conventional RC Frames", ***Emerging Science Journal***, Vol. 2, No. 3, (2018), 140-147. DOI: 10.28991/esj-2018-01137
19. Zhang, N. H. and Xing, J. J., "An alternative model for elastic bending deformation of multilayered beams", ***Journal of Applied Physics***, Vol. 100, No. 10, (2006), 103519.1-103519.5. DOI: 10.1063/1.2372578
20. Hsueh, C. H., "Thermal stresses in elastic multilayer systems", ***Thin Solid Films***, Vol. 418, No. 2, (2002), 182-188. DOI: 10.1016/S0040-6090(02)00699-5
21. Hsueh, C. H., "Stress distribution and curvature in graded semiconductor layers", ***Journal of Crystal Growth***, Vol. 258, No. 3-4, (2003), 302-309. DOI: 10.1016/S0022-0248(03)01563-X
22. Hsueh, C. H., and Lee, S., "Modeling of elastic thermal stresses in two materials joined by a graded layer", ***Composites Part B-Engineering***, Vol. 34, No. 8, (2003), 747-752. DOI: 10.1016/S1359-8368(03)00088-X
23. Chuang, T. J. and Lee, S., "Elastic flexure of bilayered beams subject to strain differentials", ***Journal of Materials Research***, Vol. 15, No. 12, (2000), 2780-2788. DOI: 10.1557/JMR.2000.0397
24. Deshpande, M. and Saggere, L., "PZT thin films for low voltage actuation: Fabrication and characterization of the transverse piezoelectric coefficient", ***Sensors & Actuators A***, Vol. 135, No. 2, (2007), 690-699. DOI: 10.1016/j.sna.2006.07.022

Persian Abstract

چکیده

در این مقاله اثر ساختارها و بارها بر روی خیز استاتیکی و مشکلات لرزش آزاد تیرهای دولایه بررسی شده است. براساس تعادل مکانیکی (استاتیکی) و تعادل انرژی، معادلات حاکم استاتیکی و دینامیکی تیر دولایه برقرار می‌شوند. مشخص شده است که مقدار نسبت ضخامت تأثیر معنی‌داری در واکنش استاتیکی و دینامیکی تیر دارد و عوامل سازه دارای اهمیت بحرانی خود هستند. هنگامی که مقدار ضخامت نسبی پایین‌تر از مقدار بحرانی آن است، یا نسبت ضخامت به طول از مقدار بحرانی آن بیشتر است، پاسخ های استاتیکی و دینامیکی تیر به وضوح افزایش می‌یابد. نتایج نشان می‌دهد که این مقدارهای بحرانی تأثیر چشم‌گیری بر خصوصیات مکانیکی تیرهای دولایه دارد. بنابراین، پژوهش‌گران در هنگام طراحی تیر دولایه باید ساختارهای بحرانی را به دقت پیش‌بینی کنند.